

From conformal to volume-law for the entanglement entropy in exponentially deformed critical spin 1/2 chains

Giovanni Ramírez,^{1,*} Javier Rodríguez-Laguna,² and Germán Sierra¹

¹*Instituto de Física Teórica UAM/CSIC, Madrid, Spain*

²*Mathematics Dept., Universidad Carlos III de Madrid, Spain*

(Dated: October 31, 2014)

An exponential deformation of 1D critical Hamiltonians gives rise to ground states whose entanglement entropy satisfies a volume-law. This effect is exemplified in the XX and Heisenberg models. In the XX case we characterize the crossover between the critical and the maximally entangled ground state in terms of the entanglement entropy and the entanglement spectrum.

I. INTRODUCTION

The ground states (GSs) of local quantum lattice Hamiltonians usually satisfy an *area law* according to which the entanglement entropy S_A of a block A of the system is proportional to the size of its boundary [1, 2]. In one spatial dimension, the area law means that S_A is bounded by a constant independent on the size of A . This statement was proved by Hasting in 2007, assuming that the Hamiltonian has finite range (locality), with finite interaction strengths and a gap in the spectrum [3]. Violations of the area law in 1D should therefore come from sufficiently non local Hamiltonians, divergent interaction strengths or gapless systems. The latter category is the most studied one and it includes translational invariant critical systems, which are described by conformal field theory (CFT), for which the gap decays with the system size L as $1/L$. In this case a logarithmic violation of the area law takes place, with a coefficient proportional to the central charge of the underlying CFT [4–6]. The area law is nevertheless restored by a massive perturbation leading to an entanglement entropy proportional to the logarithm of the correlation length in the scaling regime [6].

In this work we investigate a much stronger violation of the area law. We deform 1D critical Hamiltonians with open boundary conditions (OBC), choosing couplings that decay exponentially outwards of both sides of the center of the chain [7]. This decrease of the couplings yields a vanishing gap in the thermodynamic limit, allowing for a violation of the area law, that turns into a volume law. If the decay of the couplings is very fast, one can use the Dasgupta-Ma renormalization group (RG) that has been applied successfully to strong disordered systems [8]. The resulting GS turns out to be a valence bond state formed by bonds joining the sites located symmetrically with respect to the center. This state was termed *concentric singlet phase* by Vitagliano et al. [7], and has a *rainbow*-like structure as illustrated in figure 1.

The role of coupling inhomogeneity in 1D quantum many-body physics has been addressed from many different points of view. Quenched disorder in the couplings gives rise to GSs, which, when averaged, resemble quantum critical states [9–13]. If the couplings change smoothly enough, they can be regarded as a position-dependent speed of propagation for the excitations, or a local gravitational potential [14]. Thus, a slow decrease of the couplings to zero can be regarded as a *horizon* [15]. Smoothed boundary conditions, in which the couplings fall to zero in the borders, have been used to reduce the finite-size effects when measuring bulk properties of the GS [16]. The opposite case, in which the couplings increase exponentially or hyperbolically, has also been studied in the literature [17–19]. Other possible violations of the area-law have been recently investigated in reference [20] by means of long-range couplings with a magnetic phase and a Fermi surface with a point of accumulation.

The aim of this work is to study the behavior of entanglement in exponentially deformed critical 1D models: XX and Heisenberg. Concretely, we will focus on the transition from the conformal to the volume law.

This article is organized as follows. In section II, we define the deformed XX model in the free fermion formulation, apply the Dasgupta-Ma RG method to construct the GS for a strong deformation and obtain the numerically exact solution for all the deformation strengths. In section III, we compute the entanglement entropy and analyze its scaling properties, inspired by CFT and the transition between the conformal to the rainbow state. In section IV, we analyze the entanglement spectrum and the deformed Heisenberg model, obtaining similar results. Finally, in section V we present the conclusions and points to further work.

* giovanni.ramirez@uam.es

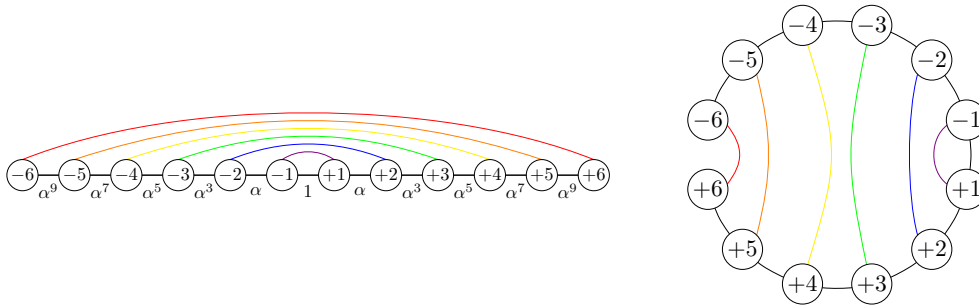


FIG. 1. (Color online) Rainbow state both in linear and circular representations, showing the $(-k, +k)$ bonds above the central link. Thus, the entanglement entropy of the left (or right) half of the chain is $L \log 2$.

II. THE MODEL

Let us consider a chain with $2L$ sites labelled by integers $i = \pm 1, \dots, \pm L$. The Hamiltonian of the model is given by

$$H_L \equiv -J_0 c_1^\dagger c_{-1} - \sum_{i=1}^{L-1} J_i \left(c_i^\dagger c_{i+1} + c_{-i}^\dagger c_{-(i+1)} \right) + \text{h.c.} \quad (1)$$

where c_i and c_i^\dagger are annihilation and creation operators of spinless fermions and J_i are the hopping amplitudes parametrized as (see figure 1)

$$\begin{cases} J_0(\alpha) = 1, \\ J_i(\alpha) = \alpha^{2i-1}, \quad i = 1, \dots, L-1 \end{cases} \quad (2)$$

Via a Jordan-Wigner transformation, the Hamiltonian (1) is equivalent to the XX model for a spin 1/2 chain. For $\alpha = 1$, one recovers the well known uniform spinless fermion model with OBC. The model with $0 < \alpha < 1$ was introduced by Vitagliano et al. to illustrate a violation of the area law for a local Hamiltonian [7]. Taking $\alpha > 1$ and truncating the chain to the sites $i = 1, \dots, L$, one obtains the Hamiltonian considered by Okunishi and Nishino, which has the scale-free property of the Wilson's numerical renormalization group of the Kondo impurity problem [17]. The models where J_i is a hyperbolic function have been considered in order to measure the energy gap [19].

The ground state of H_L can be studied by means of two different methods: Dasgupta-Ma RG and exact diagonalization. The former provides a valence bond picture of the GS in the limit $\alpha \rightarrow 0^+$, which explains in simple terms the volume law. On the other hand, the second method is applicable to all values of α and in particular to the limit $\alpha \rightarrow 1^-$, where one recovers the uniform model, with a log law described by CFT. We shall show that the two limits are connected continuously, that is, with no phase transitions between them. This fact offers the possibility of studying the crossover between the log law and the volume law of the entanglement entropies, which exhibits interesting features.

1.- Renormalization Group. In the Dasgupta-Ma RG method, one selects the strongest link between two nearest neighbor sites and places a bonding state between them [8]

$$|\Psi\rangle = \frac{1}{\sqrt{2}} (|10\rangle + |01\rangle). \quad (3)$$

The two sites are then removed from the chain and an effective coupling is established between the two sites that border the newly created bond. The hopping amplitude for this effective link is found using second order perturbation theory:

$$\tilde{J}_i = \frac{J_{i-1} J_{i+1}}{J_i}. \quad (4)$$

In the framework of tensor networks, this renormalization step can be seen as a disentangler operation between the sites contained in the bond [21]. In our case, that is $\alpha < 1$, the strongest link is the central one. A bond is thus established on top of link J_0 , between sites -1 and $+1$ and an effective hopping is established between sites -2 and $+2$, with strength

$$\tilde{J}_{-2,+2} = \frac{J_{+1} J_{-1}}{J_0} = \alpha^2. \quad (5)$$

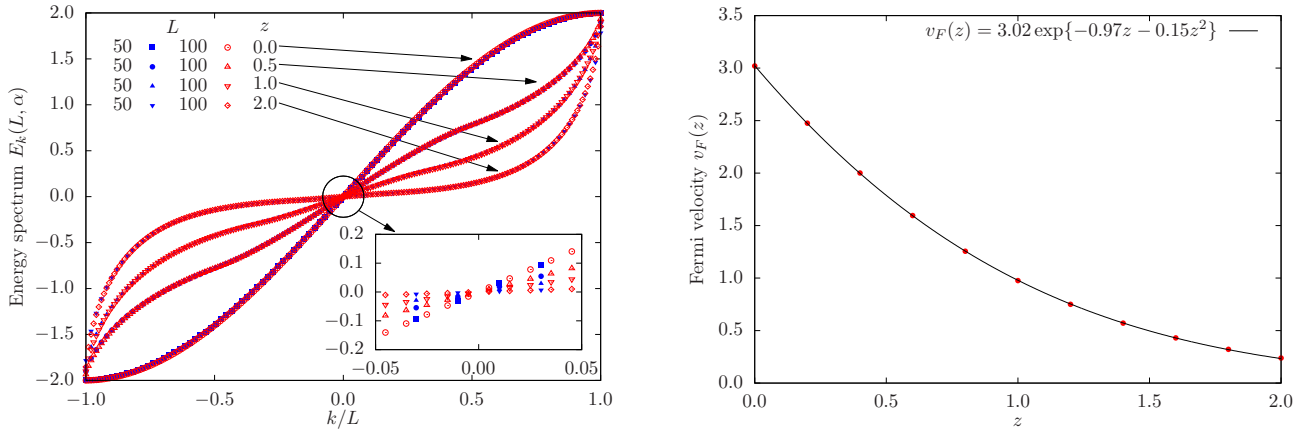


FIG. 2. Left: Energy spectrum $E_k(L, \alpha)$ for $L = 50, 100$ and several values of z . The data collapse on the same curve, which shows the scaling law (9). Right: Fermi velocity $v_F(z)$ as a function of z . The solid line is an exponential fit.

This newly created link is again the strongest one, since $\alpha^2 > \alpha^3$, so we establish a new bond between sites -2 and $+2$ (figure 1, blue bond), and renormalize the coupling between sites -3 and $+3$ as α^4 . The procedure repeats itself, until the $2L$ sites are linked by L valence bond states, whose shape looks like a *rainbow*. It is easy to see that after the first RG state one can factor out an overall constant α^2 in the couplings J_i , such that the renormalized Hamiltonian becomes $\alpha^2 H_{L-1} + \text{const}$. This fact implies that the rainbow state is a trivial fixed point of the RG with zero correlation length between nearest neighbor sites, except the sites $i = \pm 1$.

In summary, the rainbow state can be written as the valence bond state:

$$|R_L\rangle = \prod_{k=1}^L |\Psi\rangle_{-k,+k}, \quad (6)$$

where $|\Psi\rangle_{-k,+k}$, given in equation (3), is a single bond, a *Bell pair* between sites $-k$ and $+k$. In that state, the reduced density matrix ρ_B of any block B has a very characteristic spectrum $\{\lambda_p\}$ [10]: if n_B is the number of bonds joining B with the rest of the system, the eigenvalue 2^{-n_B} appears with multiplicity 2^{n_B} . Thus, the von Neumann entropy can be easily computed: $S(B) \equiv -\sum \lambda_k \log \lambda_k = n_B \log 2$, i.e. the number of broken Bell pairs multiplied by $\log 2$. Moreover, all Rényi entropies take the same value. Within the RG approximation, the entanglement properties of the GS are independent of α . The validity of the renormalization scheme improves when the renormalized link is much stronger than the surrounding ones, that is $\alpha \ll 1$. Thus, one can assert that the rainbow state becomes the exact GS of the H_L Hamiltonian in the limit $\alpha \rightarrow 0^+$.

Let B be the block containing half of the chain, so $n_B = L$. Its entanglement entropy is straightforward to compute: $L \cdot \log 2$; i.e. the state is maximally entangled and fulfills a volume law. The energy gap can be estimated as the effective energy of the last bond established, which scales as α^{2L} and for $\alpha < 1$ vanishes in the limit $L \rightarrow \infty$ in agreement with the Hastings theorem. For use later, we shall define the following quantity

$$z = -L \log \alpha, \quad (7)$$

in terms of which $\alpha^{2L} = e^{-2z}$. Notice that z can be endowed with a physical interpretation as the ratio between L and the decay length of the hopping amplitudes. We shall see below that z plays the role of a scaling parameter in the limit $L \gg 1$ and $\alpha \approx 1$.

2.- Exact Diagonalization. The Hamiltonian (1) is quadratic in the fermionic operators. Therefore its spectrum can be obtained by diagonalizing the corresponding $2L \times 2L$ hopping matrix $T_{ij} = -J_0 \delta_{ij,-1} - J_i \delta_{|i-j|,1}$, $i, j = \pm 1, \dots, \pm L$. One can easily verify that if ϕ_i is an eigenfunction with energy E , then $(-1)^i \text{sign}(i) \phi_i$ is another eigenfunction with energy $-E$. Thus the GS of the chain is obtained by filling the lowest energy levels with L fermions (half-filling). The eigenmodes, ϕ_i^k , fulfill $T_{ij} \phi_j^k = E_k \phi_i^k$. We shall choose the label of the eigenfunctions as $k = 0, \pm 1, \dots, \pm(L-1), -L$, such that the particle-hole symmetry becomes $E_k = -E_{-k-1}$ and $E_k < E_{k+1}$. In the uniform case, i.e. $\alpha = 1$, one obtains $E_k = 2 \sin[\pi(2k+1)/(2(2L+1))]$. The GS of the chain is given by

$$|R(\alpha)\rangle = \prod_{k=-1}^{-L} d_k^\dagger(\alpha) |0\rangle, \quad (8)$$

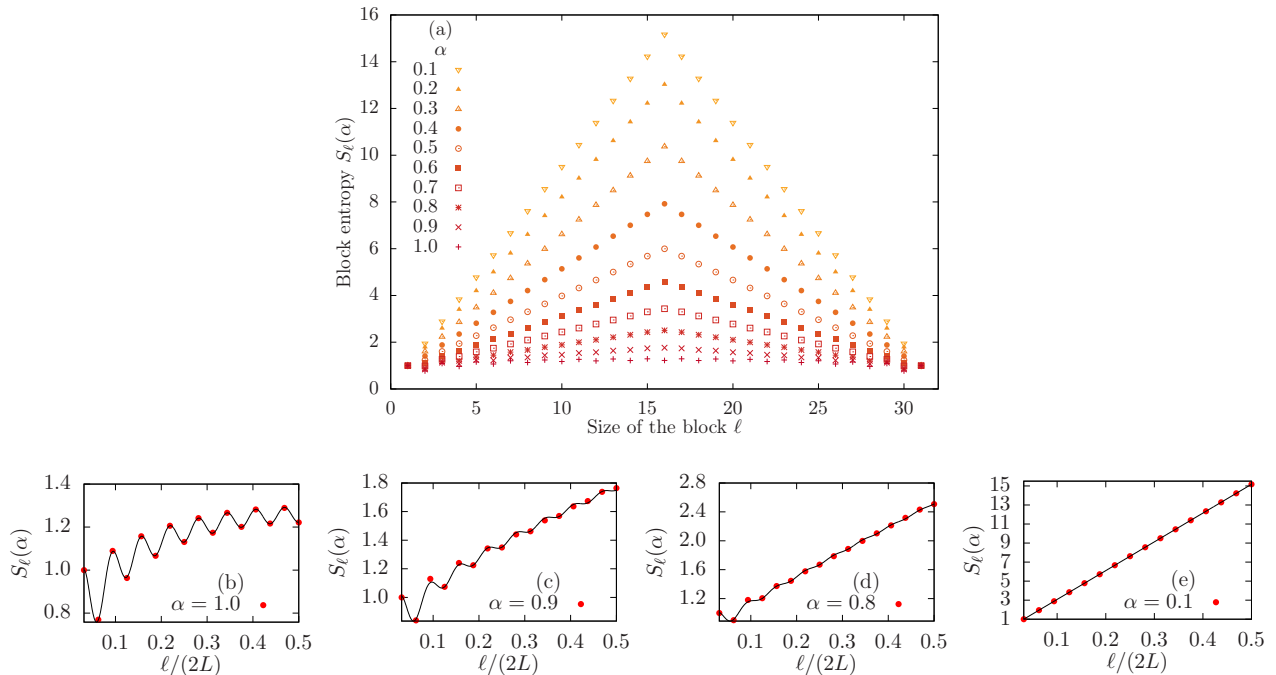


FIG. 3. (a) Block entropy $S_\ell(\alpha)$, for a system of size $L = 16$ (32 sites). Notice the *tent shape* for small α , denoting volumetric growth of the entanglement entropy. (b) For the uniform case $\alpha = 1$; (c) for $\alpha = 0.9$; (d) for $\alpha = 0.8$ and (e) for $\alpha = 0.1$.

where $d_k^\dagger = \sum_i \phi_i^k c_i^\dagger$. We have not found closed analytic expressions for the eigenvalues and eigenfunctions when $\alpha \neq 1$, but some general properties can be obtained numerically. In particular, the spectrum $E_k(L, \alpha)$ satisfies the scaling law

$$E_k(L, \alpha) \simeq e_z(k/L), \quad k, L \gg 1, \quad (9)$$

which is illustrated in the left panel of figure 2. The dispersion relation e_z changes smoothly from the *sine* function, for $z \ll 1$ to an almost flat function near the origin for $z \gg 1$. At half-filling the relevant modes lie in the neighborhood of Fermi point where the dispersion relation linearizes,

$$e_z(k/L) \simeq v_F(z)k/L, \quad k/L \ll 1, \quad (10)$$

with a Fermi velocity $v_F(z)$ (see right panel of figure 2).

III. ENTANGLEMENT ENTROPY

The entanglement properties are found from equation (8) [22]. Let B be a block of size ℓ , and let $i, j \in B$. Then the two point-correlator of the fermion operators c_i is given by

$$C_{ij}^B = \langle R(\alpha) | c_i^\dagger c_j | R(\alpha) \rangle = \sum_{k=-1}^{-L} \bar{\phi}_i^k(\alpha) \phi_j^k(\alpha). \quad (11)$$

Let $\{\nu_p\}_{p=1}^\ell$ be its eigenvalues, then the reduced density matrix of the block can be written as $\rho_B = \otimes_{p=1}^\ell \rho_p$, where

$$\rho_p = \nu_p b_p^\dagger b_p + (1 - \nu_p) b_p b_p^\dagger, \quad (12)$$

for some fermionic operators b_p^\dagger . The values $\nu_p = \langle b_p^\dagger b_p \rangle$ are interpreted as *occupations* of the different modes b_p^\dagger . The von Neumann entropy of B is given by

$$S(B) = - \sum_{p=1}^\ell [\nu_p \log \nu_p + (1 - \nu_p) \log(1 - \nu_p)]. \quad (13)$$

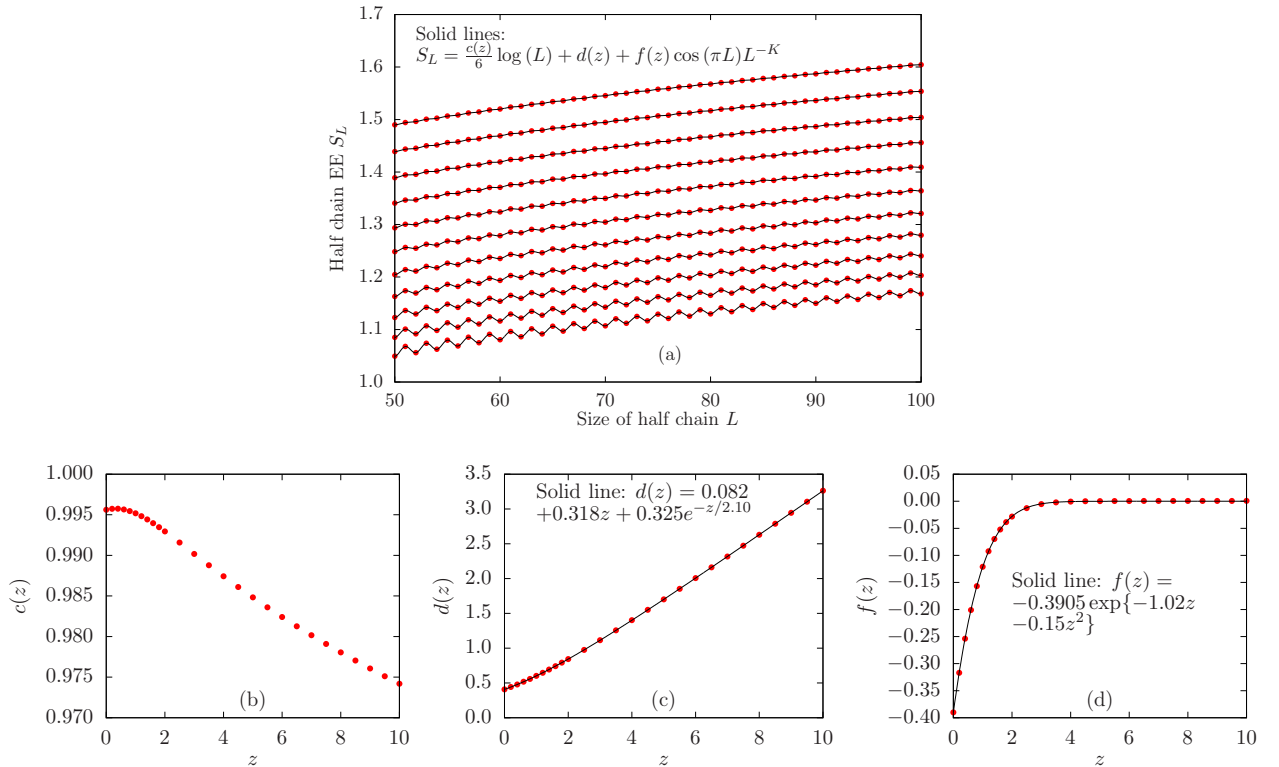


FIG. 4. (a) Half-chain entanglement entropy S_L as a function of the system half size $L = 50, \dots, 100$ for $z = 0$ to 2 in steps of 0.2 from bottom to top. Solid lines are fits to (14) with $\chi^2 \sim 10^{-10}$. The data corresponding to the values $2 < z \leq 10$, not shown in this figure, also satisfy equation (14). (b)-(d) Functions $c(z)$, $d(z)$ and $f(z)$, in the interval $z \in [0, 10]$, together with fits for $d(z)$ and $f(z)$.

The set $\{\nu_p\}$ allows a full computation of the entanglement spectrum, i.e. the spectrum of the reduced density matrix ρ_B , which provides the most complete information about entanglement and can help characterize quantum phase transitions[23].

We should remark that the numerical computation of the eigenstates of matrix T_{ij} is an ill-conditioned problem if z is large. Working at double precision the upper bound for z can be estimated as $e^{-2z_{\max}} \sim 10^{-16}$, that is $z_{\max} \sim 18$, but we shall be usually working below this value.

Let $S_\ell(\alpha)$ denote the von Neumann entropy of the block containing the leftmost ℓ sites in the GS. Figure 3(a) shows its dependence with ℓ for different values of α in a system with $L = 16$, i.e. with 32 sites. For low values of α we observe a characteristic *tent shape*, i.e. an approximately linear growth up to $\ell = L$ followed by a symmetric linear decrease, giving the volumetric behavior. As α grows, the slope decreases and ripples start to appear. These numerical data can be fitted to a formula that contains linear, oscillating and logarithmic functions of ℓ with coefficients that depend in a non trivial manner in α and L .

To simplify the analysis of the functional dependence of the entropy on these parameters, we shall consider the von Neumann entropy of the half-chain, $S_L(\alpha)$. Figure 4(a) shows the values of S_L for $L = 50, \dots, 100$ and fixed values of $z = 0, \dots, 2$ (note that α is tuned with L in order to keep z constant). Quite remarkably the half-chain entropy can be fitted to the expression

$$S_L = \frac{c(z)}{6} \log L + d(z) + f(z) \cos(\pi L) L^{-K}, \quad (14)$$

where the functions $c(z)$, $d(z)$ and $f(z)$ are shown in figures 4(b)-(d) respectively, together with the corresponding fits. The Luttinger parameter K in equation (14) is taken equal to 1, which gives the best fit to the numerical data. Equation (14) is motivated by the standard CFT formulas recovered in the case $z = 0$, which corresponds to a CFT with central charge $c = 1$ and Luttinger parameter $K = 1$ [5, 6, 24–26].

Indeed, in the limit $z \rightarrow 0$, we obtain $c(z) \rightarrow 0.995$. As z increases, the function $c(z)$ decreases. This result reminds us of the Zamolodchikov c -theorem, according to which a certain function C of the coupling constants of a relativistic $1 + 1$ quantum field theory, never increases along the RG flow and equals the central charge of the CFT at the fixed points [27, 28]. In our case, there is a fixed point at $z = 0$, which corresponds to a free fermion with OBC which has

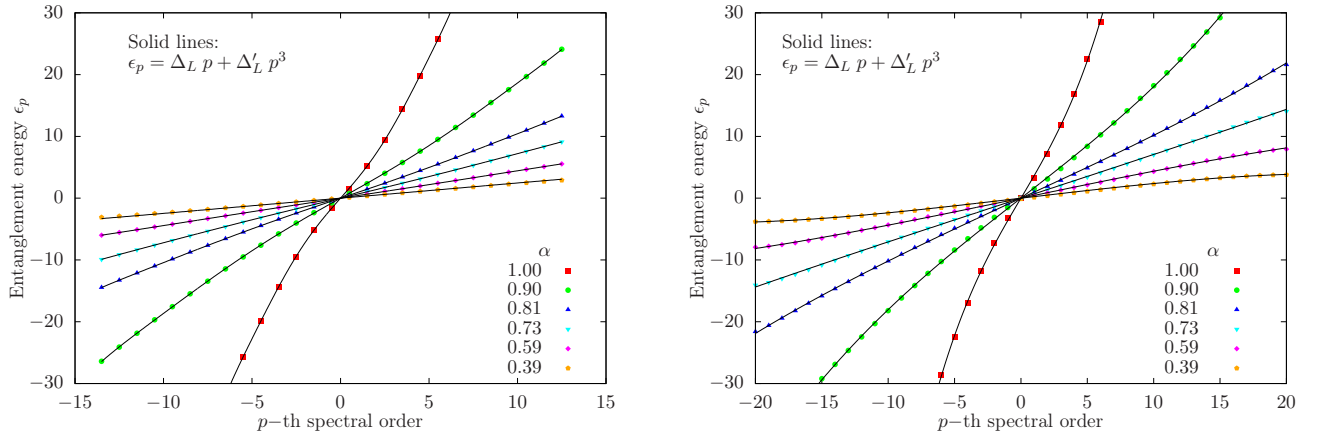


FIG. 5. Entanglement energies of the half-chain for several values of α and $L = 40$ (left) and $L = 41$ (right) together with a fit to the equation (19).

$c = 1$. One should expect that along the RG flow the value of z increases while $c(z)$ decreases, approaching zero in the limit $z \rightarrow \infty$, where one finds the rainbow state, which is a trivial fixed point of the RG.

Let us next discuss the term $d(z)$ in equation (14). In a CFT on a strip of length $2L$, the entanglement entropy of the half line is given by $S_L = c/6 \log(2L/\pi) + c'_1 + 2g + f \cos(\pi L)L^{-K}$ [6, 24–26], where g is the boundary entropy of Affleck and Ludwig [29]. We may then interpret $d(z)$ as a z dependent boundary entropy $g(z)$, up to some non universal constants. As the c -theorem, the g -theorem asserts that the g function decreases under the RG flow of the boundary, so long as the bulk theory remains critical during the boundary flow [30, 31]. However, there are no reasons for this behavior if the bulk theory also flows with the RG [32]. This is the situation found here, where $d(z)$ increases with z , as shown in figure 4(c). The linear increase of $d(z)$ is responsible for the extensive behavior of the entanglement entropy and can be understood from the Dasgupta-Ma RG in the large z regime, or $\alpha \ll 1$.

The last term in equation (14) describes the oscillations of S_L , which are clearly visible in figure 4(a) for $z \leq 1$. This behavior is due to the function $f(z)$, which vanishes for $z \simeq 2$ as shown in figure 4(d).

We can use equation (14) to study the limit $L \gg 1$ with α kept constant, which implies $z \gg 1$. From figures 4(b)-(d) one finds that $c(z) \rightarrow 0$, $d(z) \rightarrow 0.318z$ and $f(z) \rightarrow 0$ so that

$$S_L \rightarrow -0.318L \log \alpha, \quad L \gg 1. \quad (15)$$

This result cannot be valid for very small α since we know that for $\alpha \rightarrow 0^+$ the entropy is given by $S_L = L \log 2$. The crossover takes place for $\alpha \sim 1/8$.

IV. ENTANGLEMENT SPECTRUM

In order to provide a thorough characterization of the entanglement of the half-chain we have analyzed its entanglement spectrum (ES) [23]. The reduced density matrix for a block can always be written as $\rho_B \equiv \exp(-H_E)$, where H_E is called the entanglement Hamiltonian. In the case where the state is a Slater determinant, such as $|R_L(\alpha)\rangle$, H_E can be expressed as a free-fermion Hamiltonian:

$$H_E = \sum_{p=1}^{\ell} \epsilon_p b_p^\dagger b_p + f_0, \quad (16)$$

where ϵ_p are the entanglement energies (EE), which can be computed from the eigenvalues $\nu_p = \langle b_p^\dagger b_p \rangle$ of the correlation matrix C_{ij}^B as

$$\nu_p = \frac{1}{1 + \exp(\epsilon_p)}. \quad (17)$$

The overall constant f_0 is given by

$$f_0 = \sum_{p=1}^{\ell} \log(1 + e^{\epsilon_p}). \quad (18)$$

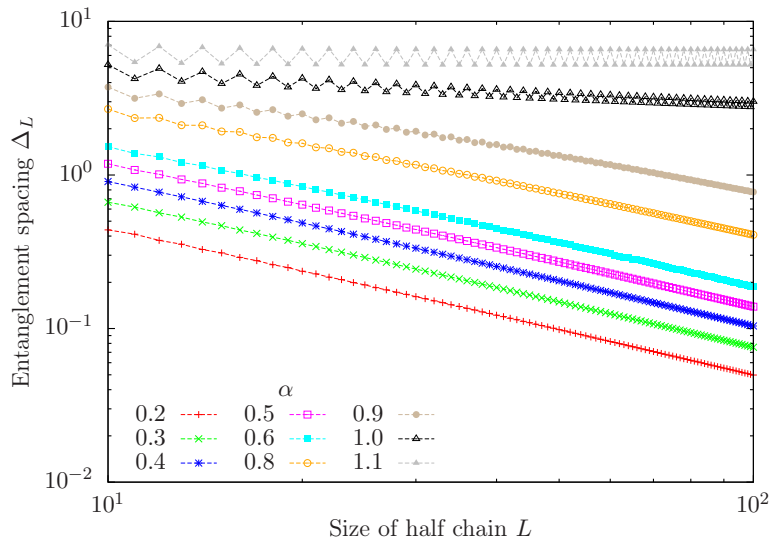


FIG. 6. Entanglement spacing Δ_L as a function of L for different values of α . Notice the behavior $\propto 1/\log L$ for $\alpha = 1$ and $\propto 1/L$ for $\alpha < 1$ and L large. The case corresponding to $\alpha = 1.1$ shows a qualitatively different behavior.

Let us consider our block to be the half-chain. In the limit $\alpha \rightarrow 0^+$, we obtain the rainbow state, which is maximally entangled and the ES is straightforward to describe. Each site makes up a bond with another site out of the block. Thus, each broken bond provides an entanglement mode, b_p^\dagger , localized at site p , with occupation probability $\nu_p = 1/2$. Applying expression (17), we can see that the entanglement energies are all $\epsilon_p = 0$. In other terms, the entanglement Hamiltonian $H_E = f_0 = L \log 2$ gives the entanglement entropy $S_L = L \log 2$.

Figure 5 shows the ES for a chain with $L = 40$ and $L = 41$, for different values of α . Note that for L odd there is a zero energy. In agreement with the previous discussion for small α , the values of ϵ_p are located around zero. However, as α increases the EE increases almost linearly in the proximity of the zero energy following the law

$$\epsilon_p \approx \Delta_L p + \Delta'_L p^3, \quad |p/L| \ll 1, \quad (19)$$

where $\Delta'_L \ll \Delta_L$, as [33]. The label p is chosen now as a half-odd integer $p = \pm 1/2, \pm 3/2, \dots, \pm(L-1)/2$ when L is even and as an integer $p = 0, \pm 1, \dots, \pm(L-1)/2$ for L odd. The EEs given by (19) correspond to the ones where $\nu_p \simeq 1/2$ which therefore contribute the most to the entanglement entropy S_L . In fact, making the approximation $\epsilon_p \approx \Delta_L p$, we can compute S_L in the limit $L \gg 1$,

$$S_L = \sum_p \left[\frac{\log(1 + e^{\epsilon_p})}{1 + e^{\epsilon_p}} + \frac{\log(1 + e^{-\epsilon_p})}{1 + e^{-\epsilon_p}} \right] \approx 2 \int_{-\infty}^{\infty} dx \frac{\log(1 + \exp(\Delta_L x))}{1 + \exp(\Delta_L x)} = \frac{\pi^2}{3 \Delta_L}. \quad (20)$$

This equation is rather interesting since it relates S_L to the inverse of the entanglement spacing Δ_L and connects with previous results in the literature [34–37]. First of all, in the critical case, that is $z = 0$, where $S_L \approx 1/6 \log L$, it implies that $\Delta_L \propto 1/\log L$, as shown in [38]. This result has wider implications that lead to the understanding of the ES as the energy spectrum of a boundary CFT on a strip of effective width $\propto \log L$ [39]. The computation in equation (20) is similar to the one of reference [6] for the non critical Ising and XXZ models, which leads to the equation $S_L = c/6 \log \xi$ where ξ is the correlation length and is proportional to the inverse of the level spacing of the spectrum of the corner transfer matrix Hamiltonian on these models.

The dependence of the entanglement spacing Δ_L on the system size L has a different behavior for $\alpha = 1$ and $\alpha < 1$. Figure 6 shows some Δ_L curves, for different values of α , in scale $\log L$. As soon as $\alpha < 1$ and large enough L we obtain a trend towards a power-law decay, which, for large L , converges to $\Delta_L \approx 1/L$. Combining this with (20), yields the volume law for the entanglement entropy: $S(L) \approx 1/\epsilon \approx L$, as expected.

Based on equations (14) and (20) we are led to the following ansatz for the entanglement spacing

$$\Delta_L \approx \frac{\pi^2/3}{\frac{1}{6}\tilde{c}(z) \log L + \tilde{d}(z) + \tilde{f}(z)L^{-\tilde{K}(z)}}, \quad (21)$$

where the functions $\tilde{c}(z)$, $\tilde{d}(z)$, $\tilde{f}(z)$ and $\tilde{K}(z)$ depend on the parity of L . This formula is extremely accurate with a χ^2 of order 10^{-12} in the range $z \in [0, 1]$. Figure 7(a) plots the values of Δ_L as a function of L for different values of

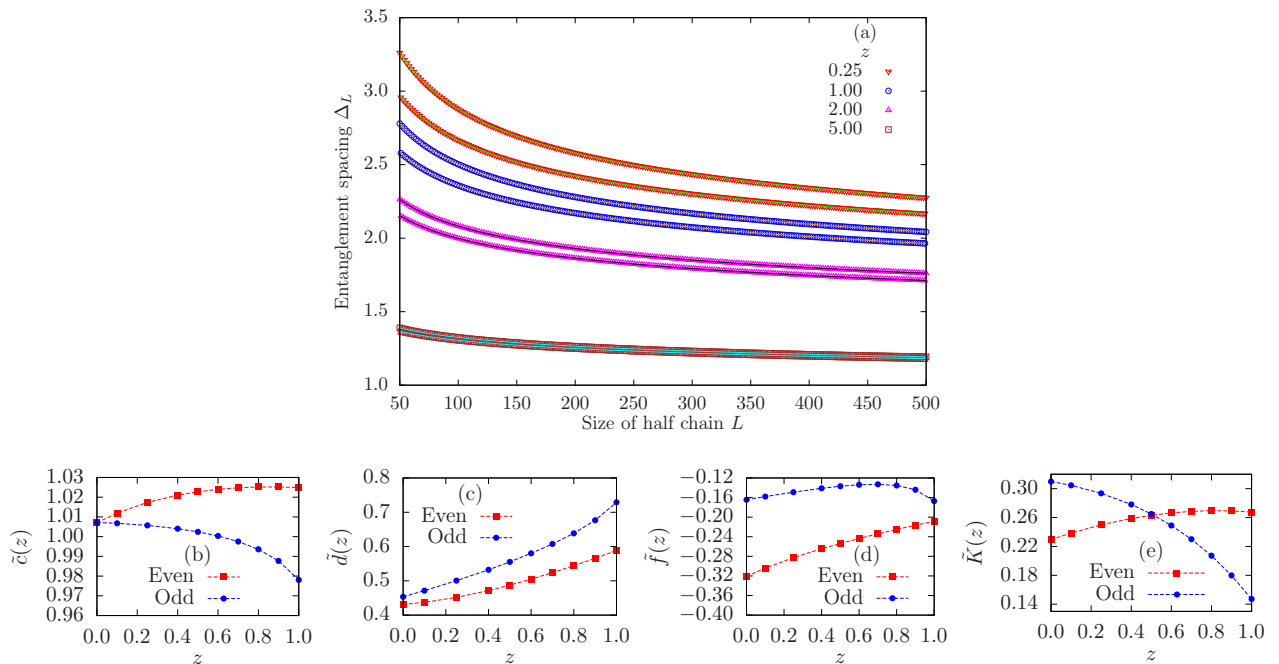


FIG. 7. (a) Entanglement spacing Δ_L as a function of the system half size $L = 50, \dots, 500$. For each value of z the top (bottom) curves correspond to L even (odd). Solid lines are fits to (21) with $\chi^2 \sim 10^{-12}$. (b)-(e) Functions $\tilde{c}(z)$, $\tilde{d}(z)$, $\tilde{f}(z)$ and $\tilde{K}(z)$, in the interval $z \in [0, 1]$ for L even (odd).

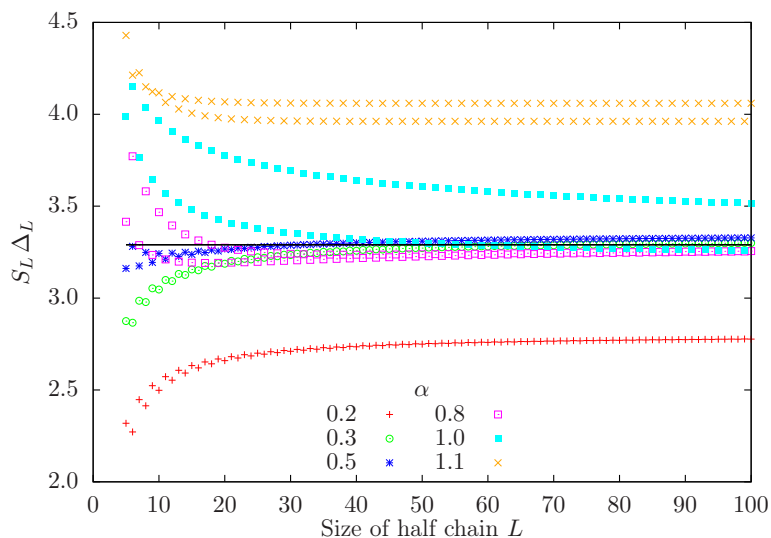


FIG. 8. Plot of the product $S_L \Delta_L$ to illustrate equation (20). The black straight line is the constant $\pi^2/3$.

z . Notice that the parity oscillations of L are reminiscent to those of S_L . The functions $\tilde{c}(z)$, $\tilde{d}(z)$ and $\tilde{f}(z)$ behave in a similar (though not identical) way to their pairs $c(z)$, $d(z)$ and $f(z)$ in the interval $z \in [0, 1]$, especially for the L even values. For larger z those fits lose quality. Notice that $\tilde{K}(z)$ is not 1, but close to 0.25.

Finally, in order to verify equation (20) we plot in figure 8 the product $S_L \Delta_L$, which shows that for $\alpha \leq 1$ the curves approach the constant $\pi^2/3$ for large values of L , but not for $\alpha = 1.1$, which corresponds to a model with different qualitative behavior.

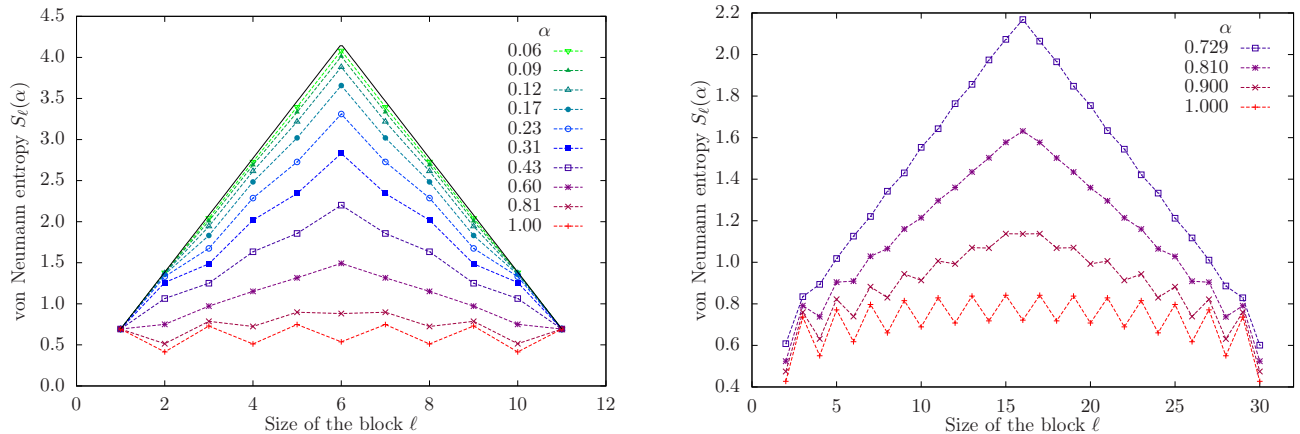


FIG. 9. Left: von Neumann entropy of the deformed Heisenberg system and $L = 6$ (12 sites), where all the values of α are explored. Right: system with $L = 16$ (32 sites) studied with the DMRG method. The fast increase of entanglement of the half-chain limits the range of α where the method can be applied.

A. The spin 1/2 deformed Heisenberg model

The deformed XX model can be immediately generalized to any 1D Hamiltonian with OBC; $H = \sum_{i=1}^{2L-1} h_{i,i+1}$, whose exponential deformation is given by

$$H_L(\alpha) = J_0(\alpha)h_{1,-1} + \sum_{i=1}^{L-1} J_i(\alpha) (h_{i,i+1} + h_{-i,-(i+1)}), \quad (22)$$

where $J_i(\alpha)$ are defined in equation (2). We shall next consider the exponential deformation of the Heisenberg Hamiltonian defined by $h_{i,i+1} = \vec{S}_i \cdot \vec{S}_{i+1}$, where \vec{S}_i are the spin 1/2 matrices. The deformed Hamiltonian easily follows from equation (22). The Dasgupta-Ma RG equation for the couplings is given by [10]

$$\tilde{J}_i = \frac{J_{i-1}J_{i+1}}{2J_i}, \quad (23)$$

which differs from equation (4) by a factor of 2 in the denominator. In the limit $\alpha \rightarrow 0$, one obtains again the rainbow state made of valence bonds across the middle of the chain.

The numerical study of the uniform to rainbow transition is more involved than in the free fermionic case, because the GS cannot be obtained via single-body procedures. For very small system sizes, we have used exact diagonalization of the many-body Hamiltonian, while for larger sizes we have employed the density matrix renormalization group (DMRG). The problem with the latter is that we cannot reach very low values of α , since the entanglement entropy S_L grows linearly with the system size and the number of retained states grows exponentially with S_L . Figure 9 summarizes our results: the left panel shows the exact von Neumann entropy as a function of the block size $S_\ell(\alpha)$ for $L = 6$ (12 sites). Notice the black line, which marks the Dasgupta-Ma RG limit. The right panel shows the same function for a system with $L = 16$ (32 sites), but where α varies in the range $[0.7, 1]$. In both cases we can see the development of the tent shape, which is the hallmark of the volume-law.

V. CONCLUSIONS

We have analyzed a deformation of critical local 1D Hamiltonians, which interpolates between a log law and a volume law for the entanglement entropy. The couplings between neighboring sites decay exponentially, with a factor α^2 , as we move away from the middle point. The value $\alpha = 1$ corresponds to the uniform model, described by CFT and in the $\alpha \rightarrow 0^+$ limit the GS becomes a rainbow state, in which sites symmetrically placed with respect to the center are maximally entangled. There is a smooth crossover between the uniform and the rainbow states that we have studied in detail for the XX model (free spinless fermions model) and shown to be qualitatively equivalent in the Heisenberg model.

In the XX model, the von Neumann entropy of any block, at not too small values of α , can be approximated by a combination of the CFT law plus a volume law. We have also found a scaling variable z that depends on the size of the

chain and the magnitude of the deformation α in terms of which the half-chain entanglement entropy is a renormalized version of the CFT formulas, with coefficients depending on z . We have discussed this result in connection with the c - and g -theorems.

The analysis of the ES shows very interesting connections between the conformal growth, $S \sim \log L$ and the volumetric growth, $S \sim L$. Indeed, the spectrum is approximately equally spaced, with an entanglement spacing Δ_L that decays with the system size as $1/\log L$ at the conformal point and as $1/L$ for $\alpha < 1$. We have also found that the entanglement entropy is approximately proportional to the inverse of the entanglement spacing, in wide regions of the parameter space, which generalizes previous known results in critical and massive systems.

In summary, we have shown that an exponential deformation of the XX and Heisenberg models offers the possibility to analyze the departure from the log law of the entanglement entropy in CFT towards a volume law that is related to the valence bond picture of these models. It would be worth to study other critical models to verify the generality of these results, as well as non critical models that will exhibit a crossover from the area to the volume law. Finally, it will be very interesting to construct the field theory underlying the exponential perturbation of CFT's that will give an explanation of the scaling behavior obtained numerically in this work [40].

VI. ACKNOWLEDGMENTS

We would like to acknowledge J I Latorre, A Trombettoni, F C Alcaraz, G Martínez and J Eisert. We also acknowledge financial support from the Spanish government from grant FIS2012-33642 and the Spanish MINECO Centro de Excelencia Severo Ochoa Programme under grant SEV-2012-0249. J R-L acknowledges support from grant FIS2012-38866-C05-1. G R acknowledges the support from grant FIS2009-11654.

-
- [1] M. Srednicki, Phys. Rev. Lett. **71**, 666 (1993).
 - [2] J. Eisert, M. Cramer, and M. B. Plenio, Rev. Mod. Phys. **82**, 277 (2010).
 - [3] M. B. Hastings, J. of Stat. Mech.: Theory and Experiment **2007**, P08024 (2007).
 - [4] C. Holzhey, F. Larsen, and F. Wilczek, Nuclear Physics B **424**, 443 (1994).
 - [5] G. Vidal, J. I. Latorre, E. Rico, and A. Kitaev, Phys. Rev. Lett. **90**, 227902 (2003).
 - [6] P. Calabrese and J. Cardy, J. of Stat. Mech.: Theory and Experiment **2004**, P06002 (2004).
 - [7] G. Vitagliano, A. Riera, and J. I. Latorre, New Journal of Physics **12**, 113049 (2010).
 - [8] C. Dasgupta and S.-k. Ma, Phys. Rev. B **22**, 1305 (1980).
 - [9] G. Refael and J. E. Moore, Phys. Rev. Lett. **93**, 260602 (2004).
 - [10] G. Refael and J. E. Moore, Journal of Physics A: Mathematical and Theoretical **42**, 504010 (2009).
 - [11] N. Laflorencie, Physical Review B **72**, 140408+ (2005).
 - [12] M. Fagotti, P. Calabrese, and J. E. Moore, Phys. Rev. B **83**, 045110 (2011).
 - [13] G. Ramírez, J. Rodríguez-Laguna, and G. Sierra, J. of Stat. Mech.: Theory and Experiment **2014**, P07003 (2014).
 - [14] O. Boada, A. Celi, J. I. Latorre, and M. Lewenstein, New Journal of Physics **13**, 035002 (2011).
 - [15] J. Rodríguez-Laguna, A. Celi, and M. Lewenstein, "work in progress," (2014).
 - [16] M. Vekić and S. R. White, Phys. Rev. Lett. **71**, 4283 (1993).
 - [17] K. Okunishi and T. Nishino, Phys. Rev. B **82**, 144409 (2010).
 - [18] H. Ueda and T. Nishino, Journal of the Physical Society of Japan **78**, 014001 (2009).
 - [19] H. Ueda, H. Nakano, K. Kusakabe, and T. Nishino, Progress of Theoretical Physics **124**, 389 (2010).
 - [20] G. Gori, S. Paganelli, A. Sharma, P. Sodano, and A. Trombettoni, ArXiv e-prints (2014), arXiv:1405.3616 [cond-mat.stat-mech].
 - [21] J. I. Cirac and F. Verstraete, Journal of Physics A: Mathematical and Theoretical **42**, 504004 (2009).
 - [22] I. Peschel, Journal of Physics A: Mathematical and General **36**, L205 (2003).
 - [23] H. Li and F. D. M. Haldane, Phys. Rev. Lett. **101**, 010504 (2008).
 - [24] N. Laflorencie, E. S. Sørensen, M.-S. Chang, and I. Affleck, Phys. Rev. Lett. **96**, 100603 (2006).
 - [25] P. Calabrese, M. Campostrini, F. Essler, and B. Nienhuis, Phys. Rev. Lett. **104**, 095701 (2010).
 - [26] M. Fagotti and P. Calabrese, J. of Stat. Mech.: Theory and Experiment **2011**, P01017 (2011).
 - [27] A. B. Zamolodchikov, Pis'ma Zh. Eksp. Teor. Fiz. **43**, 565 (1986), [JETP Lett. **43** 730-732 (1986)].
 - [28] J. Cardy, *Scaling and Renormalization in Statistical Physics*, Cambridge Lecture Notes in Physics (Cambridge University Press, 1996).
 - [29] I. Affleck and A. W. W. Ludwig, Phys. Rev. Lett. **67**, 161 (1991).
 - [30] I. Affleck and A. W. W. Ludwig, Phys. Rev. B **48**, 7297 (1993).
 - [31] D. Friedan and A. Konechny, Phys. Rev. Lett. **93**, 030402 (2004).
 - [32] D. Green, M. Mulligan, and D. Starr, Nuclear Physics B **798**, 491 (2008).
 - [33] V. Eisler and I. Peschel, J. of Stat. Mech.: Theory and Experiment **2013**, P04028 (2013).

- [34] I. Peschel and T. Truong, *Zeitschrift für Physik B Condensed Matter* **69**, 385 (1987).
- [35] J. L. Cardy and I. Peschel, *Nuclear Physics B* **300**, 377 (1988).
- [36] K. Okunishi, *Journal of the Physical Society of Japan* **74**, 3186 (2005).
- [37] L. Lepori, G. De Chiara, and A. Sanpera, *Phys. Rev. B* **87**, 235107 (2013).
- [38] I. Peschel, *J. of Stat. Mech.: Theory and Experiment* **2004**, P06004 (2004).
- [39] A. M. Läuchli, *ArXiv e-prints* (2013), arXiv:1303.0741 [cond-mat.stat-mech].
- [40] G. Ramírez, J. Rodríguez-Laguna, and G. Sierra, “work in progress,” (2014).